# Chronic microsensors for longitudinal, subsecond dopamine detection in behaving animals

Jeremy J Clark[1,4], Stefan G Sandberg[1,4], Matthew J Wanat[1], Jerylin O Gan[1,2], Eric A Horne[1], Andrew S Hart[1,2], Christina A Akers[1], Jones G Parker[3], Ingo Willuhn[1], Vicente Martinez[1], Scott B Evans[1], Nephi Stella[1,2] & Paul E M Phillips[1,2]

**Neurotransmission operates on a millisecond timescale but is changed by normal experience or neuropathology over days to months. Despite the importance of long-term neurotransmitter dynamics, no technique exists to track these changes in a subject from day to day over extended periods of time. Here we describe and characterize a microsensor that can detect the neurotransmitter dopamine with subsecond temporal resolution over months *in vivo* in rats and mice.**



The mesencephalic dopamine systems are a primary focus of research into motor control, motivation and reinforcement learning[1,2], and their disruption is implicated in many neurological and neuropsychiatric disorders, including Parkinson's disease, schizophrenia, substance abuse and depression[3,4]. In particular, much attention focuses on the subsecond electrophysiological responses of dopamine neurons to behaviorally relevant stimuli including primary rewards, reward-predicting cues and new objects[1]. Consequently, the detailed characterization of the activity of dopamine neurons and ensuing dopamine release in target structures has been and continues to be a highly active and important area of research.

Chemical approaches are necessary to directly assess extracellular dopamine dynamics in target structures[5]. Classic neurochemical techniques, such as microdialysis, are ideal for measuring tonic baseline levels of neurotransmitters such as dopamine but have low sampling rates (minutes) and thus cannot temporally resolve the rapid changes in extracellular dopamine concentration predicted by neurophysiological data. However, electrochemical techniques, such as fast-scan cyclic voltammetry (FSCV), can provide the necessary high temporal resolution detection. FSCV offers chemical selectivity to discriminate dopamine from other electroactive species in the brain by providing an electrochemical signature (cyclic voltammogram) of the analyte. This methodology is used to detect subsecond changes in behaviorally evoked dopamine release after the presentation of salient stimuli and during behavioral tasks[6–8]. However, existing approaches are constrained by the requirement for acute implantation of a voltammetric probe into the brain via a microdrive for each experiment[9], limiting the ability to track longitudinal changes in neurotransmitter dynamics over the course of disease progression in animal models or throughout most learning paradigms[10]. Conversely, previous attempts to use chronically implanted electrodes to make long-term electrochemical measurements have had limited success[11–13]. These studies conclude that the fidelity of chemical recordings can be severely impaired by perturbation of the microenvironment through physical tissue disruption and/or neuroinflammation, emphasizing that size and biocompatibility are critical considerations in the design of chronic devices for *in situ* neurochemistry[14,15].

Here we describe a biocompatible voltammetric microsensor that can be chronically implanted into the targets of midbrain dopamine systems where it can detect subsecond dopamine dynamics from day to day over periods of months. This microsensor consists of a 7-µm-diameter carbon fiber housed in a 90-µm-diameter polyimide-covered fused-silica capillary (**Fig. 1a**). These microsensors produced a linear response to physiological concentrations of dopamine as assessed *in vitro* with flow-injection analysis ($n = 5$, $r^2 = 0.92$, $P < 0.0001$; **Fig. 1b**).

To determine the biocompatibility and suitability for long-term chemical recordings, we assessed the expression of glial markers and tyrosine hydroxylase using immunohistochemistry after chronic microsensor implantation. We prepared striatal slices from rats implanted with microsensors for 10–16 weeks and

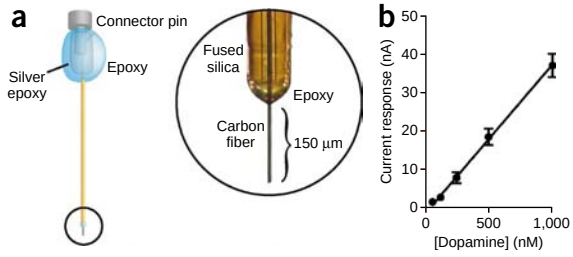


**Figure 1** | Chronic carbon-fiber microsensor. (**a**) Schematic of the chronic microsensor, which consisted of a carbon fiber encased in a polyimide-fused silica. To ensure electric insulation, a two-component epoxy was applied to the fused silica–carbon fiber interface. At the opposite end, a female pin connector was electrically connected to the carbon fiber with silver epoxy. Finally, two-component epoxy was used to coat the connector for electrical insulation and structural integrity. (**b**) The response of the microsensor to physiological concentrations of dopamine ($n = 5$). Error bars, ± s.e.m.

[1]Department of Psychiatry and Behavioral Sciences and Department of Pharmacology, [2]Graduate Program in Neurobiology and Behavior and [3]Department of Biochemistry, University of Washington, Seattle, Washington, USA. [4]These authors contributed equally to the work. Correspondence should be addressed to P.E.M.P. (pemp@uw.edu).

RECEIVED 8 SEPTEMBER; ACCEPTED 24 NOVEMBER; PUBLISHED ONLINE 27 DECEMBER 2009; DOI:10.1038/NMETH.1412

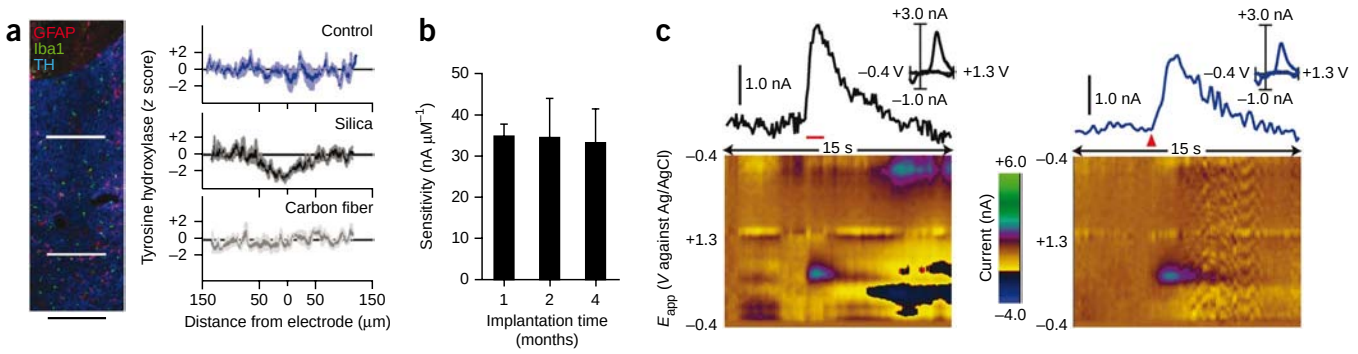


**Figure 2** | *In vivo* fidelity of chronic carbon-fiber microsensors. (**a**) Wide-field fluorescence image of a 30-μm striatal slice (left) shows immunohistochemical staining for astrocytes (GFAP), microglia (Iba1) and tyrosine hydroxylase (TH) at a microsensor tract ending ventral to the anterior commissure (dark area at the top of the image) with no apparent gliosis present. Scale bar, 300 μm. Line scans (right) of TH intensities across the fused-silica tract (top white line in fluorescence image) and the carbon-fiber tract (bottom white line in fluorescence image), presented as *z* scores (dark line, mean; shaded area, s.e.m.; $n = 5$). (**b**) Microsensor sensitivity to dopamine, assessed by flow injection analysis, after one ($n = 5$), two ($n = 5$) or four ($n = 4$) months of implantation. Error bars, ± s.e.m. (**c**) Voltammetric signal and corresponding background-subtracted cyclic voltammogram (inset) in response to stimulation (60 Hz, 24 pulses at 120 μA; red bar) of the ventral tegmental area (left) or in response to reward delivery (right; red triangle) in the same rat and on the same day. The pseudocolor plots depict color-coded observed changes in redox currents as a function of applied potential (*y* axis) plotted over time (*x* axis).



stained the slices for markers of microglia (Iba1) and astrocytes (glial fibrillary acidic protein; GFAP). We detected dopamine *in vivo* at four of the five implantation sites tested. We found no glial encapsulation near the tract left by the 7-μm carbon fiber (**Fig. 2a**) in agreement with previous studies demonstrating that probes less than 12 μm in diameter are not encapsulated[15]. In some slices, we detected a few reactive astrocytes near the fused-silica shaft, as indicated by an increase in GFAP staining (**Supplementary Fig. 1**), and a small number of dispersed activated microglia, as evident by their condensed morphology. However, even around the tract left by the shaft, glial encapsulation was not evident. In comparison to control tissue, we found that tyrosine hydroxylase immunostaining was decreased along the tract left by the fused silica shaft but not at the site of the carbon fiber (**Fig. 2a** and **Supplementary Fig. 1**). No differences in gliosis or tyrosine hydroxylase staining were noted between the implantation sites of the four functional microsensors and that of the single microsensor that did not detect dopamine. Lack of dopamine detection in apparently healthy tissue is not surprising given previous findings demonstrating the heterogeneity in behaviorally evoked dopamine signals in the striatum[16]. Together, these results demonstrate that chronic implantation of the carbon fiber for up to 4 months did not result in overt reactive gliosis, encapsulation of the carbon fiber or a loss of tyrosine hydroxylase expression, any of which could affect chemical detection.

To determine the stability of microsensor sensitivity during implantation, we extracted electrodes from 14 rats after 1–4 months in the brain and tested microsensor sensitivity to dopamine in the flow-injection apparatus *in vitro*. Dopamine sensitivity was not significantly different between microsensors that had been implanted for 1, 2 or 4 months ($F_{2,11} = 0.012$, $P = 0.99$; **Fig. 2b**) and was similar to that for microsensors that had not previously been implanted (**Fig. 1b**) indicating stability during chronic implantation for up to 4 months.

Next we tested the ability of the chronically implanted microsensor to detect dopamine *in vivo*. The functionality of a voltammetry electrode can be assessed by measuring fluctuations in dopamine release after electrical stimulation of the ventral tegmental area (VTA), substantia nigra pars compacta or the medial forebrain bundle[6]. Using the chronically implanted microsensor, we detected electrically evoked dopamine release in the nucleus accumbens, and it was comparable to that obtained with acute voltammetry electrodes in this work (**Fig. 2c**) and in previous reports[6]. FSCV is known to confer temporal distortion to *in vivo* dopamine signals[17]. However, we noted that there was more temporal distortion in the response from the chronically implanted microsensor compared to an acutely implanted electrode (**Supplementary Fig. 2**). Although this process does not impair the detection of changes in phasic signaling amplitude during learning or in disease models, mathematical deconvolution procedures may be useful for quantitatively precise kinetic analysis[17].

Electrically evoked neurochemical signals provide a reliable means to assess the functionality of specific recording electrodes, but behaviorally evoked signals, such as reward presentation, are often more experimentally relevant. Delivery of natural rewards has been shown to increase the firing of dopamine neurons in the VTA and substantia nigra pars compacta in monkeys[1] and elicits dopamine release in the nucleus accumbens in rats[7]. The chronic microsensor was also effective at detecting dopamine release to this type of stimulus (**Fig. 2c**). The cyclic voltammogram corresponding to the food-evoked signal was significantly correlated with an electrically evoked signal from the same microsensor ($r^2 \geq 0.75$, $P < 0.0001$; **Fig. 2c**), indicating that the behaviorally evoked signal is reliably identified as dopamine by established signal identification methods (cyclic voltammogram analysis). In addition, a comparison of cyclic voltammograms obtained *in vitro* and under a variety of conditions *in vivo* revealed a significant correlation for all observations ($r^2 \geq 0.75$, $P < 0.0001$; **Supplementary Fig. 3**). This relationship was similar to that for acute electrode preparations (**Supplementary Fig. 3**). The behaviorally evoked signal could be attenuated by inactivation of the VTA, the primary dopamine innervation to the nucleus accumbens, thus validating the signal (**Supplementary Fig. 4**). Collectively this electrochemical and pharmacological characterization together with the anatomical, physiological and independent verification

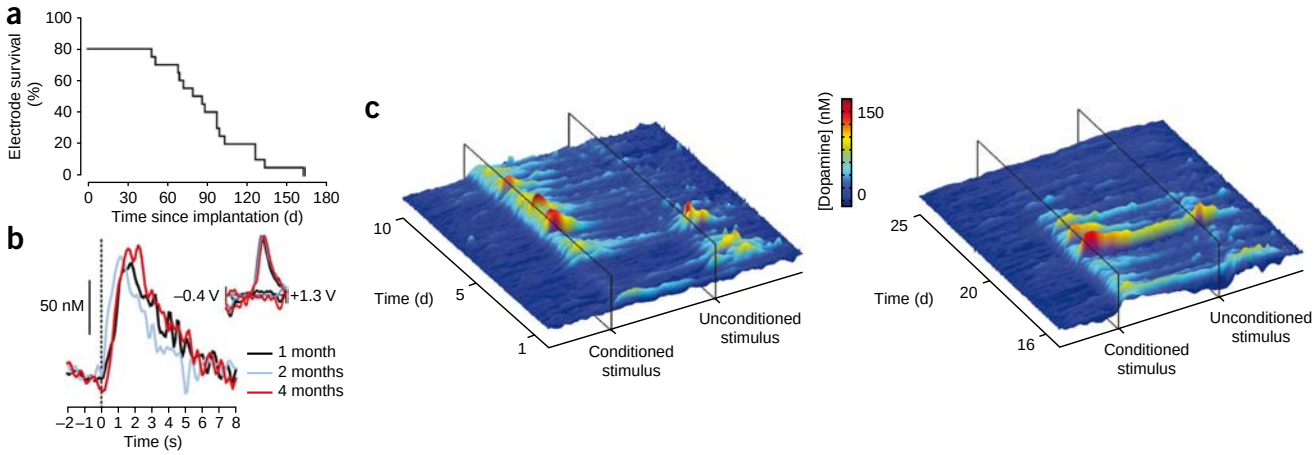


**Figure 3** | Long-term fidelity of chronic microsensors *in vivo*. (**a**) A survival curve depicting the attrition rate of chronic microsensors as a function of time after implantation. A microsensor was classified as 'viable' if an electrochemical signal elicited by reward delivery met criterion for dopamine where it was statistically correlated with a background-subtracted cyclic voltammogram obtained from electrically evoked dopamine ($r^2 \geq 0.75$). (**b**) Voltammetric signals in response to reward delivery (dashed line) at indicated times after implantation. Inset, electrochemical signature for dopamine. (**c**) Voltammetric signals in response to reward delivery (unconditioned stimulus) and a predictive cue (conditioned stimulus) during Pavlovian conditioning. The surface plots show trial-by-trial fluctuations in dopamine concentration during the 20-s period around reward and cue presentation during acquisition (days 1–10, left), a period when the reward value was increased from one to four food pellets (days 16–20, right), and extinction (days 21–25, right) in a representative rat.

(**Supplementary Note**) provides a high degree of confidence that the recorded signal is that of dopamine.

To assess the longevity of dopamine detection with this approach, we chronically implanted 20 microsensors and repeatedly tested their ability to detect behaviorally evoked dopamine release, verified by cyclic voltammogram analysis (**Fig. 3a**). There are several potential sources of electrode attrition relevant to maintaining chronic recordings; therefore, we included all electrodes in the analysis regardless of their failure mode (**Supplementary Table 1**). Four microsensors failed before dopamine detection. The remaining 16 microsensors could detect dopamine for 1.5–4 months after surgery.

We reliably detected behaviorally evoked dopamine release in the nucleus accumbens 1, 2 and 4 months after implantation (**Fig. 3b**). Cyclic voltammograms obtained from reward-evoked dopamine release at these time points and those obtained from electrically evoked release at 1 and 2 months after surgery were significantly correlated with each other and those obtained *in vitro* ($r^2 \geq 0.75, P < 0.0001$; **Supplementary Table 2**). This maintained fidelity *in vivo* is consistent with the demonstration that microsensor sensitivity is stable over months after implantation. Finally, we monitored electrochemical signals during multiple-day reinforcement learning to demonstrate the potential of combining a chronically implantable microsensor with FSCV in assessing the dynamics of phasic dopamine release events over time. A specific role for dopamine in reinforcement learning is suggested by data from numerous paradigms[2]. Indeed, previous work with FSCV has demonstrated phasic dopamine release events in response to primary rewards and their predictors[8]. However, a complete characterization of phasic dopamine events in response to conditioned and unconditioned stimuli throughout learning has remained elusive because of methodological constraints[10], which can be overcome by our approach. We plotted fluctuations in dopamine concentration recorded in the nucleus accumbens by the chronic microsensor during every trial during 25 d of training on a Pavlovian conditioned approach task in a representative rat (**Fig. 3c**). These data illustrate the trial-by-trial shift in phasic dopamine responses from reward presentation to a predictive cue during acquisition (days 1–5) and a persistent cue response during extended training (days 6–10). The capacity to sample from the same subject throughout all behavioral manipulations reveals the modulation of reward-evoked responses by changes in reward value (increased reward days 16–20) and the attenuation of cue-evoked responses during extinction (reward omission days 21–25).

The advantage of our approach is in the ability to obtain multiple, repeated recordings in a single subject over a period of days, weeks or months. In addition to the assessment of the neurochemical correlates of psychological processes such as learning and memory, research aimed at exploring dopamine in animal models of psychiatric or neurological disorders will benefit from the capacity to measure during all aspects of the modeled disorder[18,19]. Although we collected the longitudinal data presented here in rats, we also used this microsensor for long-term, *in vivo* neurochemical measurements in mice (**Supplementary Fig. 3**). The now widely used manipulation of the mouse genome makes this an attractive species for the study of disease processes. Finally, our approach also permits the simultaneous assessment of dopamine release in multiple brain nuclei in a single subject (**Supplementary Fig. 5**), a manipulation not possible with currently available methodology. These additional applications have the potential to extend the already rich field of *in vivo* voltammetry and allow researchers to make new inquiries and approach long-standing questions in a new way.

## METHODS

Methods and any associated references are available in the online version of the paper at http://www.nature.com/naturemethods/.

*Note: Supplementary information is available on the Nature Methods website.*

**ACKNOWLEDGMENTS**

We thank S. Barnes for technical assistance and M. Walton and W. Shain for useful discussions. This work was supported by the University of Washington Royalties Research Fund and the US National Institutes of Health (R01-MH079292 to P.E.M.P.; R21-DA024140 to P.E.M.P.; and R01-DA014486 to N.S.). J.J.C. was supported by F32-DA024540, M.J.W. was supported by T32-AA007455 (to M. Larimer), J.O.G. was supported by T32-GM007270 (to D. Kimelman), and A.S.H., J.G.P. and E.A.H. were supported by T32-DA007278 (to C. Chavkin).

**AUTHOR CONTRIBUTIONS**

P.E.M.P. conceived the work; S.B.E. optimized the microsensor design; J.J.C., S.G.S., N.S. and P.E.M.P. designed experiments and prepared the manuscript; J.J.C., S.G.S., M.J.W., J.O.G., E.A.H., A.S.H., J.G.P., C.A.A., I.W. and V.M. collected and analyzed data.

**COMPETING INTERESTS STATEMENT**

The authors declare no competing financial interests.

**Published online at http://www.nature.com/naturemethods/.**
**Reprints and permissions information is available online at http://npg.nature.com/reprintsandpermissions/.**

1. Schultz, W., Dayan, P. & Montague, P.R. *Science* **275**, 1593–1599 (1997).
2. Wise, R.A. *Neuron* **36**, 229–240 (2004).
3. Hornykiewicz, O. & Kish, S.J. *Adv. Neurol.* **45**, 19–34 (1987).
4. Nestler, E.J. & Carlezon, W.A. *Biol. Psychiatry* **59**, 1151–1159 (2006).
5. Montague, P.R. *et al. J. Neurosci.* **24**, 1754–1759 (2004).
6. Phillips, P.E.M., Stuber, G.D., Heien, M.L., Wightman, R.M. & Carelli, R.M. *Nature* **422**, 614–618 (2003).
7. Roitman, M.F., Stuber, G.D., Phillips, P.E.M., Wightman, R.M. & Carelli, R.M. *J. Neurosci.* **24**, 1265–1271 (2004).
8. Day, J.J., Roitman, M.F., Wightman, R.M. & Carelli, R.M. *Nat. Neurosci.* **10**, 1020–1028 (2007).
9. Phillips, P.E.M., Robinson, D.L., Stuber, G.D., Carelli, R.M. & Wightman, R.M. in *Drugs of Abuse: Neurological Reviews and Protocols* (ed., Wang, J.Q.) 443–464 (Humana Press, Totowa, New Jersey, USA, 2003).
10. Owesson-White, C.A., Cheer, J.F., Beyene, M., Carelli, R.M. & Wightman, R.M *Proc. Natl. Acad. Sci. USA* **105**, 11957–11962 (2008).
11. Kruk, Z.L. *et al. J. Neurosci. Methods* **79**, 9–19 (1998).
12. Duff, A. & O'Neill, R.D. *J. Neurochem.* **62**, 1496–1502 (1994).
13. Wilson, G.S. & Johnson, M.A. *Chem. Rev.* **108**, 2462–2481 (2008).
14. Szarowski, D.H. *et al. Brain Res.* **983**, 23–35 (2003).
15. Seymour, J.P. & Kipke, D.R. *Biomaterials* **28**, 3594–3607 (2007).
16. Wightman, R.M. *et al. Eur. J. Neurosci.* **26**, 2046–2054 (2007).
17. Venton, B.J., Troyer, K.P. & Wightman, R.M. *Anal. Chem.* **74**, 539–546 (2002).
18. Martin, S.J., Grimwood, P.D. & Morris, R.G. *Annu. Rev. Neurosci.* **23**, 649–711 (2000).
19. Tolias, A.S. *et al. J. Neurophysiol.* **98**, 3780–3790 (2007).

## ONLINE METHODS

**Microsensor fabrication.** Dopamine microsensors for chronic implantation consisted of carbon-fiber microelectrodes insulated in a fused-silica capillary[20,21]. A single carbon fiber (grade 34-700; Goodfellow Corporation) was inserted into a 10–15-mm length of fused silica (Polymicro Technologies) while submerged in 2-propanol. One end of the microsensor was then sealed with Devcon two-component epoxy (IWT Performance Polymers) and allowed to dry, leaving a length of carbon fiber protruding. A silver connector was secured in contact with the carbon fiber on the other end of the silica with silver epoxy (MG Chemicals), allowed to cure overnight then insulated with a layer of two-component epoxy. After an additional 12 h of drying, the fabrication of the chronic microsensor was finalized by trimming the exposed carbon fiber to the desired length of the sensor (150–200 μm).

**Electrochemical instrumentation.** During voltammetric analysis, analyte electrolysis is driven by applying an electrical potential via an electrode, and chemical information is provided in the ensuing current, measured at the electrode. For all recordings, the applied potential to the microsensor was held at –0.4 V versus Ag/AgCl between voltammetric scans and then ramped to +1.3 V and back at 400 V $s^{-1}$ during the scan (8.5 ms total scan time). Voltammetric scans were repeated every 100 ms to obtain a sampling rate of 10 Hz. When dopamine is present at the surface of the electrode during a voltammetric scan, it is oxidized during the anodic sweep to form dopamine-*o*-quinone (peak reaction at approximately +0.7 V) which is reduced back to dopamine in the cathodic sweep (peak reaction at approximately –0.3 V). The ensuing flux of electrons is measured as current and is directly proportional to the number of molecules that undergo the electrolysis. For the chemical identification of dopamine, current during a voltammetric scan can be plotted against the applied potential to yield a cyclic voltammogram. The cyclic voltammogram provides a chemical signature that is characteristic of the analyte, allowing resolution of dopamine from other substances. For quantification of changes in dopamine concentration over time, the current at its peak oxidation potential can be plotted for successive voltammetric scans. Waveform generation, data acquisition and analysis were carried out on a PC-based system using two multifunction data acquisition cards and software written in LabView (National Instruments). Signals were transmitted from chronically implanted microsensors to the data acquisition system via a head-mounted voltammetric amplifier (current-to-voltage converter) and an electrical swivel (Crist Instrument Co.) mounted above the recording chamber. The voltammetric amplifier consisted of an operational amplifier with a feedback resistor ($R_f$; 5 M), which determined the current-to-voltage 'gain' (following Ohm's law: $V_{out} = I_{in} \times R_f$). In addition, a capacitor (6 pF) was connected in parallel with the feedback resistor to filter high frequencies, whereas other capacitors bridged each of the power sources (+15 V, –15 V) with ground to filter operational amplifier noise. As reported elsewhere[22], there is commonly a 200 mV shift in the reference potential at implanted Ag/AgCl electrodes. This change can be diagnosed by the position of Faradaic peaks within the background current and, when observed, the applied potential was offset by 200 mV to compensate, as previously described[23].

**Assessment of electrode sensitivity.** The sensitivity of the microsensor to dopamine was determined *in vitro* before and/or after 1, 2 and 4 months implantation in brain using flow injection analysis. Briefly, the microsensor was placed in a flowing stream of artificial cerebrospinal fluid (ACSF; 3 ml $min^{-1}$) and electrochemical measurements were made with FSCV using the same parameters used for *in vivo* recordings. A time-dependent square pulse of dopamine (dissolved in ACSF) was introduced into the flow stream via an injection valve (Upchurch Scientific). The sensitivity of the microsensor was determined by dividing the change in the voltammetric signal during introduction of dopamine by its concentration.

**Voltammetry surgery.** All animal procedures presented in this paper followed the University of Washington Institutional Animal Care and Use Committee guidelines. Surgical preparation for *in vivo* voltammetry used aseptic technique. Male rats weighing 300–350 g (Charles River) were anesthetized with isoflurane and placed in a stereotaxic frame. The scalp was swabbed with 10% povidone iodine, bathed with a mixture of lidocaine (0.5 mg $kg^{-1}$) and bupivicaine (0.5 mg $kg^{-1}$), and incised to expose the cranium. Holes were drilled and cleared of dura mater above the nucleus accumbens core (1.3 mm lateral and 1.3 mm rostral from bregma), the dorsolateral striatum (4.3 mm lateral and 1.2 mm rostral from bregma) and/or the nucleus accumbens shell (0.8 mm lateral and 1.2 mm rostral from bregma) for microsensors, above the midbrain (1.0 mm lateral and 5.2 mm caudal from bregma) for a stimulating electrode in some rats, and at convenient locations for a reference electrode and three anchor screws. The reference electrode and anchor screws were positioned and secured with cranioplastic cement, leaving the stimulating electrode and working electrode holes exposed. The microsensors were then attached to the voltammetric amplifier and lowered into the target recording regions (7.0 mm ventral of dura mater for nucleus accumbens and 4.0 mm ventral of dura mater for dorsolateral striatum). For rats in which a stimulating electrode was implanted, the voltammetric waveform was applied at 10 Hz and dopamine monitored. Next, the stimulating electrode (Plastics One) was lowered 7.0 mm below dura mater and electrical stimulation (60 biphasic pulses, 60 Hz, ± 120 μA and 2 ms per phase) was applied via an optically isolated, constant-current stimulator (A-M Systems). If an evoked change in dopamine concentration was not observed at the working electrode, the stimulating electrode was positioned 0.2 mm more ventrally. This was repeated until dopamine efflux was detected after stimulation. The electrode was then lowered in 0.1-mm increments until dopamine release was maximal. This is usually when the stimulating electrode is 8.4 mm ventral from dura mater. Finally, cranioplastic cement was applied to the part of the cranium that is still exposed to secure the stimulating electrode and microsensor(s).

**Recording sessions.** *In vivo* experiments were carried out in a standard operant chamber (Med Associates). A subset of rats was trained on a conditioned Pavlovian approach (autoshaping) task. Each trial in an autoshaping session consisted of an 8-s presentation of a lever or light cue (conditioned stimulus) followed immediately by the delivery of a food pellet (unconditioned stimulus). Each training session (one per day) was comprised of 25 trials presented on a 60-s variable-interval schedule. After 15 sessions of standard training, the reward value was increased from 1 to 4 food pellets for 5 d followed by 5 d of extinction training during which food reward was omitted.





doi:10.1038/nmeth.1412

**Pharmacological validation.** Rats were implanted with chronic, carbon fiber microsensors targeted at the nucleus accumbens core (1.3 mm lateral and 1.3 mm rostral from bregma) and with bilateral guide cannulae (26 gauge; Plastics One) directed at the VTA (0.5 mm lateral and –5.6 mm caudal to bregma and lowered 7.0 mm ventral from dura mater). Dummy cannulae (Plastics One) were installed in the guide cannulae and removed during testing. On test days (~2 months after implantation), injectors (33 gauge; Plastics One) were inserted through the guide cannulae so they protruded 1 mm beyond the guide cannulae to a final depth of 8.0 mm ventral from dura mater. Injections of 0.5 µl of ACSF (154.7 mM $Na^+$, 2.9 mM $K^+$, 132.49 mM $Cl^-$ and 1.1 mM $Ca^{2+}$ at pH 7.4) or 0.5 µl of baclofen (50 ng) dissolved in ACSF were visually monitored for accuracy and were completed within 4 min. Dopamine responses to reward delivery were recorded immediately before injections and 5 min after injections. Voltammetric responses were analyzed by calculating the area under the curve of the change in current at the peak dopamine oxidation potential which was normalized to the percentage of that for the pre-injection reward delivery.

**Multisite recording under anesthesia.** For proof of principle of recording at more than two electrodes, multisite recordings were carried out simultaneously at four acutely implanted microsensors (identical construction to the chronic microsensor) in anesthetized rats during terminal surgery. Rats were anesthetized with urethane (1.5 g $kg^{-1}$, intraperitoneally) and immobilized in stereotaxic frame. Body temperature was maintained with a deltaphase heating pad (Braintree Scientific). A midsagittal incision was placed slightly anterior and posterior of bregma and lambda, respectively. Connective tissue was removed to allow holes to be drilled (1.3 mm anterior and 1.3, 2.3, 3.3 and 4.3 mm lateral of bregma). Upon careful removal of dura mater microsensors were lowered to 7.0, 6.0, 5.0 and 4.0 mm ventral of the pial surface. In addition, a hole for stimulating electrode placement was made 4.6 mm posterior to and 1.3 mm lateral of bregma. For optimal dopamine release, the stimulating electrode was lowered at 0.1 mm increments starting at 7.0 mm until release was observed at all four microsensors. Electrically evoked dopamine was elicited by a 60-Hz, 120-pulse train with 4-ms wide bi-phasic square pulses at 300 µA (optically isolated and constant current). After completion of experiment, positions of microsensors were histologically verified.

**Histological verification of recording sites.** On completion of experimentation, rats were deeply anesthetized with intraperitoneal ketamine (100 mg $kg^{-1}$) and xylazine (20 mg $kg^{-1}$) and were then transcardially perfused with saline. The skull was carefully removed so that the attached microsensor remained intact. The brain was then removed and post-fixed in paraformaldehyde for 24 h and then rapidly frozen in an isopentane bath (~5 min). The brain was then blocked, sliced on a cryostat (50-µm coronal sections, 20 °C) and placed on slides. Slices were stained with cresyl violet to aid visualization of anatomical structures and the microsensor was localized by following the tract made by the fused-silica shaft. In a subset of rats, an electrolytic lesion (300 V) was made by applying current directly through the recording microsensor for 20 s to expedite histological identification of the recording site. However, lesioning typically alters the microsensor surface prohibiting accurate post-implantation assessment of *in vivo* sensitivity.

**Data analysis.** Electrochemical data was analyzed using software written in LabView (National Instruments). All statistical analyses were carried out using Prism (GraphPad Software). For every recording session, the chemical signature of behaviorally evoked phasic dopamine release was statistically compared to an *in vivo* template of dopamine. These templates were obtained from electrically evoked dopamine release after stimulation of the VTA or medial forebrain bundle taken from an early recording session. Behaviorally evoked signals met electrochemical criterion for dopamine if the cyclic voltammogram was closely correlated with that of stimulated release ($r^2 \geq 0.75$)[24].

**Immunohistochemistry.** Seven male, Sprague-Dawley rats each with a microsensor that had been implanted 10–16 weeks earlier were perfused and fixed with 4% paraformaldhyde. Their brains were cryoprotected (15% sucrose for 24 h followed by 30% sucrose until they sank) and were stored at –80 °C. Serial coronal sections (30 µm) were cut on a cryostat and stored in phosphate-buffered saline (PBS; 4 °C for up to 24 h). For each rat, at least three consecutive sections were selected in which the electrode tract was visually identified close to the target structure. Two additional coronal slices rostral to the electrode tract were selected for secondary-only control and image analysis (see below). Slices were washed in PBS (3 times at room temperature (25 °C)), blocked and permeablized with PBS supplemented with both donkey serum (5%) and Triton X-100 (1%) (under gentle agitation, 90 min at room temperature). Slices were then incubated under gentle agitation for 18–24 h at 4 °C with primary antibodies prepared in PBS supplemented with donkey serum (2.5%) and Triton X-100 (0.5%) at the appropriate final concentrations as follows: antibody to Iba-1 (rabbit immunoglobulin gamma, 1:400; Wako), antibody to GFAP (chicken IgY, 1:600; Millipore), antibody to tyrosine hydroxylase (mouse immunoglobulin gamma, 1:1,000; Millipore), donkey anti-rabbit Alexa Fluor 488 (1:500; Invitrogen), donkey anti-chicken Texas Red (1:125; Fitzgerald Industries International, Inc.) and donkey anti-mouse Alexa Fluor 647 (1:500; Invitrogen). For each rat, one control slice did not receive any primary antibody (for secondary-only control). Slices were then washed six times with PBS supplemented with Tween-20 (0.05%) (10 min each at room temperature), and incubated with the appropriate secondary antibodies prepared in PBS supplemented with donkey serum (2.5%) and Triton X-100 (0.5%) (1 h at room temperature). Slices were then washed six times with PBS supplemented with Tween-20 (0.05%) (under gentle agitation at room temperature, 10 min each), followed by a brief wash in distilled water. All slices from the same rat were mounted onto a charged slide (Fisher brand Superfrost/Plus; Fisher Scientific) and allowed to dry for 18–24 h. Cover slips were mounted with Vectashield (Vector Labs) and sealed with nail polish.

**Microscopy and image analysis.** Fluorescence images were collected using a Zeiss Axio Observer Z1 equipped with a pan-apochromatic × 10 (*z*-dimension stack images at 3.42 µm) using Axiovision software. Identical exposure settings were used for the experimental, nontract control and secondary-only controls. Intensities for tyrosine hydroxylase were measured at two levels in Axiovision: 100-µm below end of the fused-silica tract (at the level of the carbon fiber) and 500-µm above the end of the

fused-silica tract. This was carried out by drawing a band, 10-pixels wide and 300-μm long, on a six *z*-dimension stack compressed image. For data presentation, compressed *z*-dimension stack images were created in Axiovision and saved as tiff files. The composite images were gated to background using the secondary-only control and the composites were aligned by hand in Photoshop (Adobe). Analysis of tyrosine hydroxylase intensity at the level of the fused silica, the carbon fiber and in control tissue was carried out by calculating *z* scores for each sample based on the mean and s.d. of control tissue.


20. Swiergiel, A.H., Palamarchouk, V.S. & Dunn, A.J. *J. Neurosci. Methods* **73**, 29–33 (1997).
21. Gerhardt, G.A. *et al. J. Neurosci. Methods* **87**, 67–76 (1999).
22. Moussy, F. & Harrison, D.J. *Anal. Chem.* **66**, 674–679 (1994).
23. Heien, M.L. *et al. Proc. Natl. Acad. Sci. USA* **102**, 10023–10028 (2005).
24. Cheer, J.F., Wassum, K.M., Heien, M.L.A.V., Phillips, P.E.M. & Wightman, R.M. *J. Neurosci.* **24**, 4393–4400 (2004).






doi:10.1038/nmeth.1412

**nature** | **methods**

# Chronic microsensors for longitudinal, subsecond dopamine detection in behaving animals

Jeremy J Clark, Stefan G Sandberg, Matthew J Wanat, Jerylin O Gan, Eric A Horne, Andrew S Hart, Christina A Akers, Jones G Parker, Ingo Willuhn, Vicente Martinez, Scott B Evans, Nephi Stella & Paul E M Phillips

Supplementary figures and text:

| | |
|---|---|
| **Supplementary Figure 1** | Microenvironment surrounding the chronic microsensor |
| **Supplementary Figure 2** | Electrically evoked dopamine release measured with acute and chronic microsensor preparations |
| **Supplementary Figure 3** | Comparison of cyclic voltammograms obtained *in vitro* and from multiple *in vivo* preparations |
| **Supplementary Figure 4** | Pharmacological validation of *in vivo* voltammetric signals |
| **Supplementary Figure 5** | Multi-site, simultaneous recording |
| **Supplementary Table 1** | Failure mode of the chronically implanted electrodes presented in Figure 2a |
| **Supplementary Table 2** | Cross-comparison of cyclic voltammograms obtained from a single animal over the course of four months *in vivo* and a dopamine standard *in vitro* |
| **Supplementary Note** | Characterization of *in vivo* voltammetric signals |

**Supplementary Figure 1. Microenvironment surrounding the chronic microsensor.**

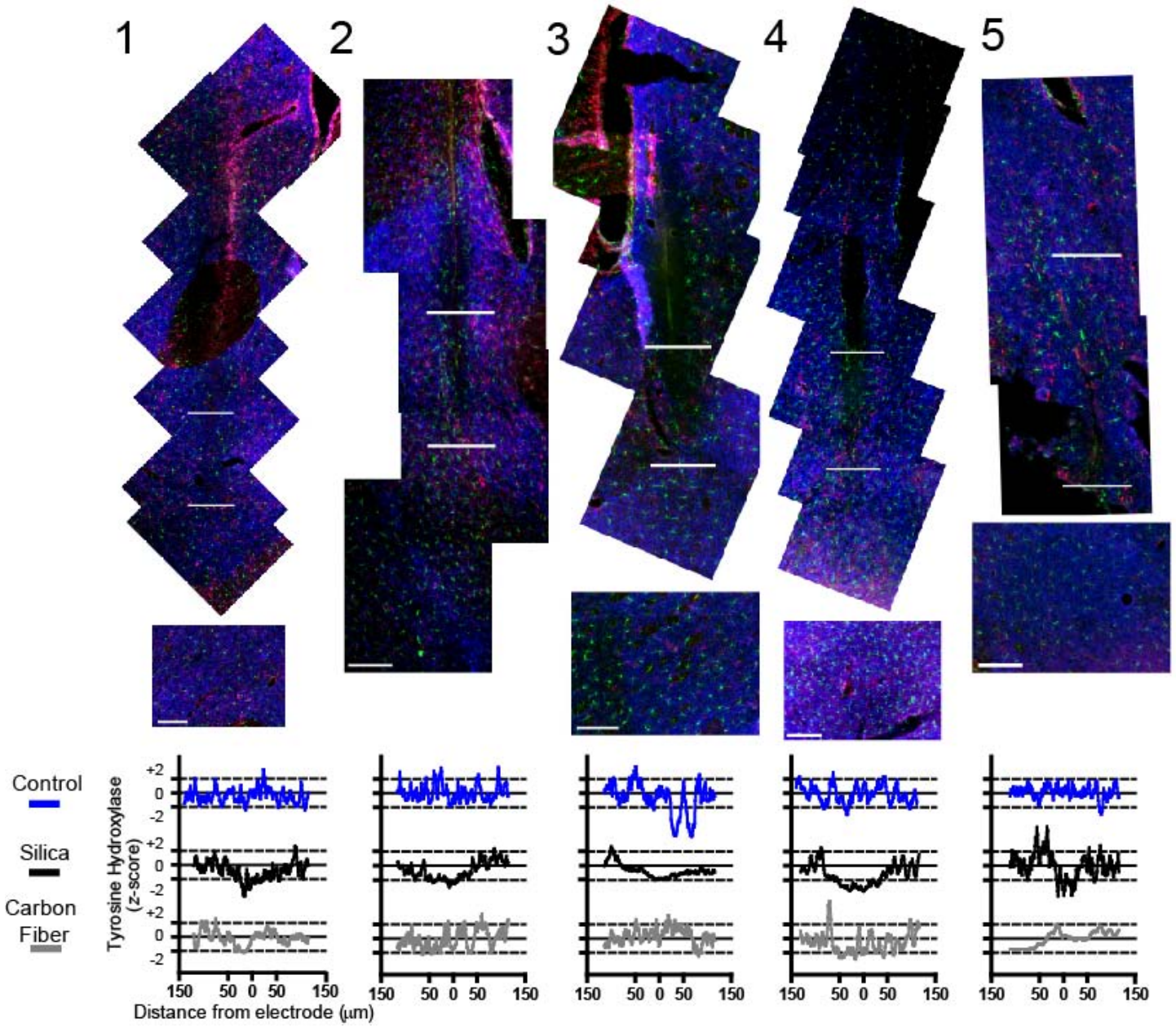


10 × composite images of 30-μm striatal sections were taken from rats implanted with a microsensor for a period of 10 to 16 weeks (*n* = 5). Striatal sections taken 1 mm anterior to the slice containing the carbon fiber were stained as a control. Astrocytes were marked with a GFAP antibody (red), microglia were labeled with the Iba1 antibody (green), and TH was used as a marker of dopaminergic synapse density (blue). While a small amount of astrogliosis is observed dorsal of the anterior commisure in the first composite image, a large astrocytic response was not observed in any of the other samples. Along the silica shaft of image 2 and 5 some activated microglia can be observed (by their condensed shape), but in all cases no glial cap is observed around the microsesnsor. The intensity of TH was measured using 300 μm line scans (150 μm radiating from the center of the silica). The middle white line in all images (100 μm below the epoxy) marks the area where TH was measured for the carbon fiber, the top white line marks the area measured for the silica shaft (500 μm from the epoxy), and the bottom white line marks the area measured for control TH expression. The five samples show significant decreases in the *z*-score of for TH intensity at the level of the silica shaft but no significant loss was observed around the carbon fiber, compared to control.



Nature Methods: doi:10.1038/nmeth.1412

**Supplementary Figure 2. Electrically evoked dopamine release measured with acute and chronic microsensor preparations.**

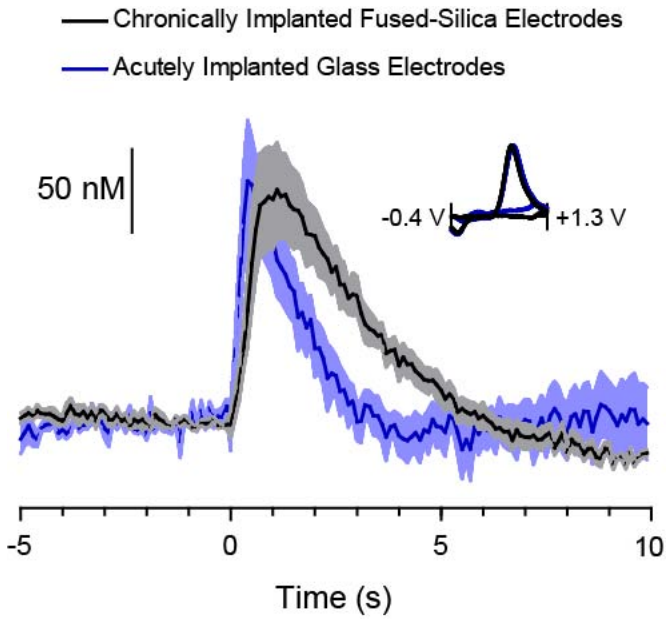


Traces depict electrically evoked dopamine release (stimulation at time 0) measured by chronic microsensors (black line $n$ = 5) and by conventional glass insulated acutely implanted electrodes (blue line $n$ = 5). Stimulating electrodes were lowered into the ventral tegmental area where electrical pulses (60 Hz, 24 pulses at 120 μA) elicited dopamine release at the recording location in the nucleus accumbens. Data are presented as mean ± s.e.m. The inset depicts the corresponding normalized background-subtracted cyclic voltammograms.



Nature Methods: doi:10.1038/nmeth.1412

**Supplementary Figure 3. Comparison of cyclic voltammograms obtained *in vitro* and from multiple *in vivo* preparations.**

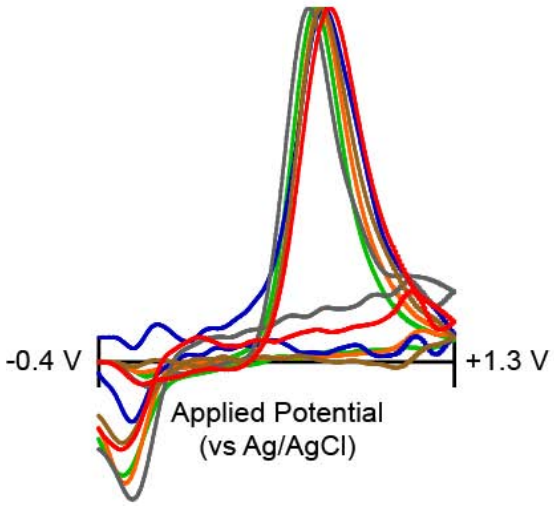


| | | | Fused-Silica Electrodes | | | | Glass Electrodes | |
|---|---|---|---|---|---|---|---|---|
| | | | Stim anesthetized | Stim waking | Reward: Rat | Reward: Mouse | Stim anesthetized | Stim waking |
| | | *In vitro* | 0.91 | 0.81 | 0.76 | 0.75 | 0.88 | 0.80 |
| Fused-Silica Electrodes | | Stim anesthetized (acute Implant) | | 0.96 | 0.92 | 0.86 | 0.98 | 0.87 |
| | | Stim waking (chronic implant) | | | 0.98 | 0.96 | 0.98 | 0.94 |
| | | Reward: Rat (chronic implant) | | | | 0.92 | 0.95 | 0.90 |
| | | Reward: Mouse (chronic implant) | | | | | 0.94 | 0.98 |
| Glass Electrodes | | Stim anesthetized (acute implant) | | | | | | 0.94 |
| | | Stim waking (acute implant) | | | | | | |

Average normalized background-subtracted cyclic voltammograms from multiple experimental preparations (left panel; $n = 5$ for each group). Statistical comparison of the average CVs obtained from each preparation revealed significant correlations between all groups (right panel; all $r^2 \geq 0.75$).



Nature Methods: doi:10.1038/nmeth.1412

**Supplementary Figure 4. Pharmacological validation of *in vivo* voltammetric signals.**

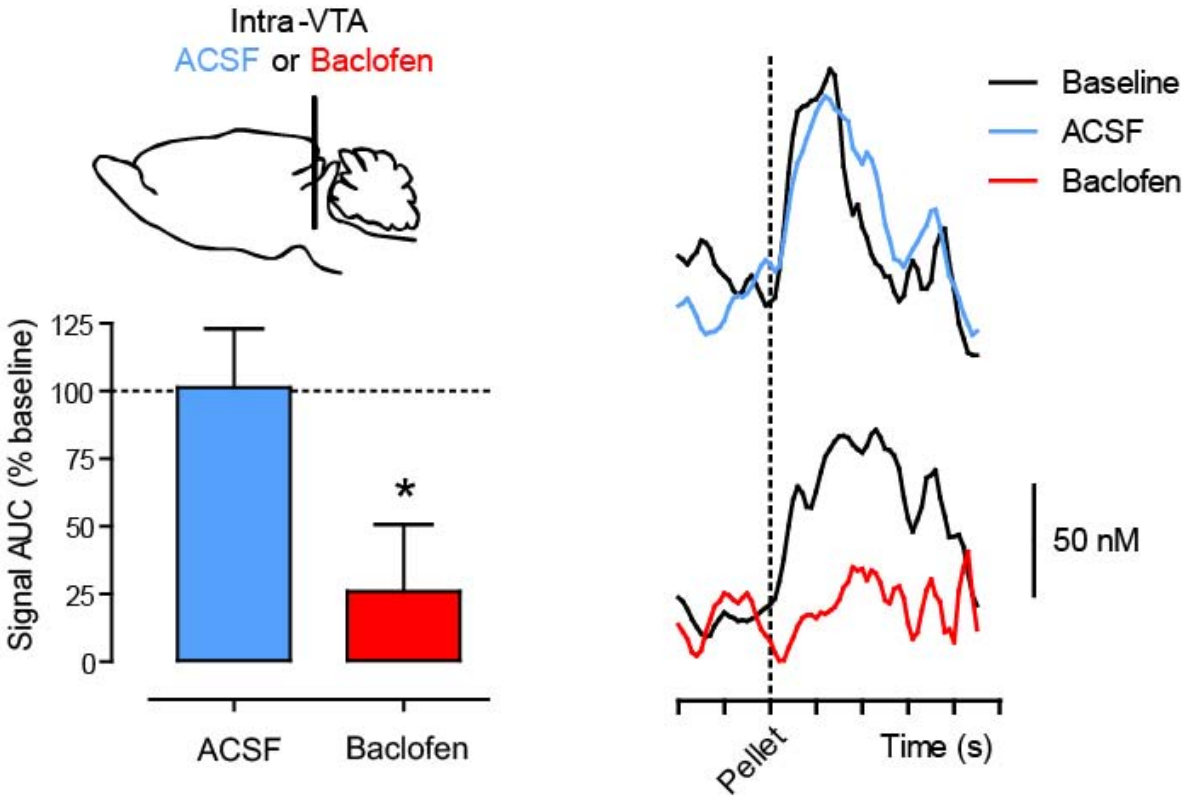


Comparison between the effect of artificial cerbrospinal fluid (ACSF; blue bar) and baclofen (50 ng; red bar) microinjections into the ventral tegmental area (VTA) on the voltammetric signal elicited by reward delivery at chronically implanted electrodes (two months after implantation). The schematic drawing depicts the saggital view of a rat brain illustrating injection sites in the VTA. Baclofen significantly reduced behaviorally evoked dopamine release in comparison to ACSF (two tailed paired t-test, $t = 3.062$, $P < 0.05$, $n = 5$; left panel). Data are presented as mean + s.e.m., normalized to pre-injection dopamine release. Representative traces of the voltammetric signal in the nucleus accumbens core from a single animal in response to reward delivery before (black) and after local microinjection of ACSF (blue) or baclofen (red) into the VTA (right panel). Each tick mark denotes one second.



Nature Methods: doi:10.1038/nmeth.1412

**Supplementary Figure 5. Multi-site, simultaneous recording.**

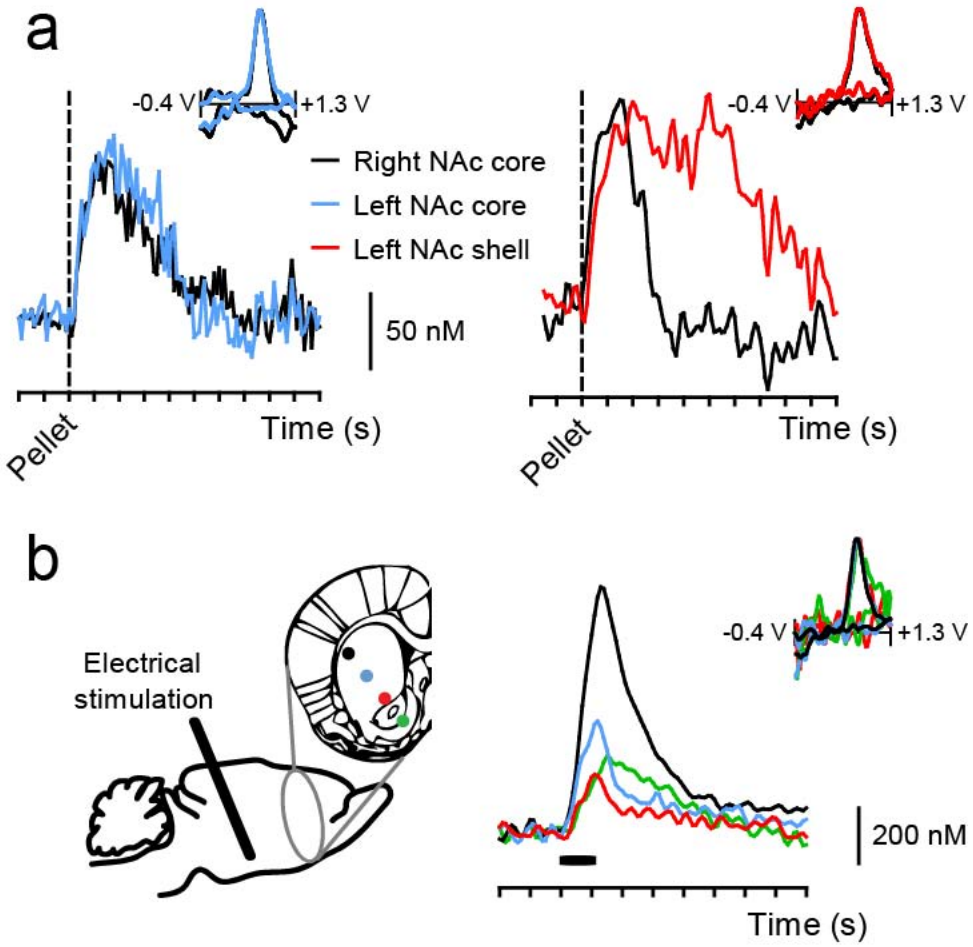


**(a)** Simultaneous recording of dopamine release in the nucleus accumbens elicited by reward presentation. The left panel shows an example of concurrent dopamine release bilaterally in the NAc core. The right panel shows an example of concurrent dopamine release in the NAc core and contralateral NAc shell. The insets depict the corresponding normalized background-subtracted cyclic voltammograms. Each tick mark denotes 1 second. **(b)** A stimulating electrode was lowered into the medial forebrain bundle where electrical pulses (60 Hz, 120 pulses at 300 μA) elicited dopamine release that was concurrently recorded in four areas of the striatum ranging from the dorsolateral striatum to the NAc. The experimental set-up is schematized and recording locations are indicated by the colored circles (left panel). Simultaneous dopamine release following electrical stimulation is shown for the four striatal locations (colored coded to indicate the recording locations depicted in the left panel) with corresponding normalized background-subtracted cyclic voltammograms in the inset (right panel). Each tick mark denotes 1 second.



Nature Methods: doi:10.1038/nmeth.1412

**Supplementary Table 1. Failure mode of the chronically implanted electrodes presented in Figure 2a.**

| Rat ID | Reason for attrition (implantation days to last successful recording*) |
|---|---|
| **1** | Separation of cranioplastic implant (79) |
| **2** | Infection around cranioplastic implant (103) |
| **3** | Increased electrical noise (88) |
| **4** | Saturated background signal after rat chewed headstage cable (133) |
| **5** | Small signal to stimulus and increased electrical drift (162) |
| **6** | Infection around cranioplastic implant (97) |
| **7** | Infection around cranioplastic implant (0†) |
| **8** | Consistent artifact following stimulus (97) |
| **9** | Infection around cranioplastic implant (86) |
| **10** | Infection around cranioplastic implant (69) |
| **11** | Intermittent electrical connection (0†) |
| **12** | Small signal to stimulus (51) |
| **13** | Intermittent electrical connection (48) |
| **14** | Consistent artifact following stimulus (72) |
| **15** | Saturated background signal (0†) |
| **16** | Consistent artifact following stimulus (126) |
| **17** | Consistent artifact following stimulus (99) |
| **18** | Separation of cranioplastic implant (126) |
| **19** | Intermittent electrical connection (68) |
| **20** | Intermittent electrical connection (0†) |

* Recording sessions were classified as successful if the electrochemical signal elicited by reward delivery met criterion for dopamine (see Methods: Data Analysis)

† Problems arose prior to or during first test that prevented subsequent recording



Nature Methods: doi:10.1038/nmeth.1412

**Supplementary Table 2. Cross comparison of cyclic voltammograms obtained from a single animal over the course of four months *in vivo* and a dopamine standard *in vitro*.**

| | **Stim, month 2** | **Reward, month 1** | **Reward, month 2** | **Reward, month 3** | ***In vitro*** |
|---|---|---|---|---|---|
| **Stim, month 1** | 0.97 | 0.96 | 0.97 | 0.92 | 0.84 |
| **Stim, month 2** | | 0.95 | 0.95 | 0.95 | 0.85 |
| **Reward, month 1** | | | 0.93 | 0.86 | 0.92 |
| **Reward, month 2** | | | | 0.91 | 0.87 |
| **Reward, month 3** | | | | | 0.81 |



Nature Methods: doi:10.1038/nmeth.1412

## Supplementary Note

*Characterization of in vivo Voltammetric Signals*

In order for the current advances in voltammetric microsensors to be experimentally useful, the microsensor and applied voltammetric technique must have the capacity to resolve and identify extracellular changes in dopamine, the primary analyte of interest. It is therefore necessary that the *in vivo* signals detected by the microsensor be adequately characterized. Four broad criteria have been proposed for the characterization of *in vivo* voltammetric signals: electrochemical, anatomical/physiological, pharmacological and independent chemical verification[1-3]. Although both FSCV and the carbon fiber used in these microsensors have already been well characterized for the detection of dopamine[1,4,5], we apply these criteria in order to evaluate our chronic microsensor and determine whether its properties are altered during chronic implantation.

The electrochemical-verification criterion can be satisfied by correlating cyclic voltammograms obtained from behaviorally evoked signals to a reference standard generated by electrical stimulation of a know source of dopamine input (VTA, SNc, or medial forebrain bundle). In FSCV, voltage is applied in a triangular waveform generating an output current profile, which when presented as a current-voltage plot (the CV) provides a chemical "signature" for the compound of interest. Correlation coefficients between CVs resulting from stimulations of the VTA, after reward presentation and exogenous dopamine standards *in vitro* are shown in **Supplementary Figure 3** for the chronically implanted microsensor and, for comparison, acutely implanted electrodes. Behaviorally evoked release was highly correlated ($r^2 \geq 0.75$) with all of the dopamine standards tested.

The second criterion, anatomical and physiological verification, can be satisfied by showing that the neurochemical of interest is present at the recording site and demonstrating that the tissue is capable of releasing the neurochemcial with the observed kinetics. All electrode placements were histologically confirmed to be in the ventral or dorsal extents of the striatum, structures previously shown by tissue measurements to be high in dopamine content[6]. In addition, immunohistological assessment of the microenvironment being sampled by the microsensor indicates that TH, the biosynthetic enzyme for dopamine, is present in the surrounding tissue (**Fig. 1b** and **Supplementary Fig. 1)**. These brain regions have been shown to support high rates of dopamine release as indicated using electrical stimulation of afferent pathways shown previously[7] and in **Figure 1c**. In addition, the dynamics and timing of data shown in **Figure 2c** from the chronically implanted microsensors are consistent with electrophysiological studies examining the firing pattern of dopamine neurons in similar behavioral paradigms[8,9]. Specifically when rewards are preceded by sensory stimuli, dopamine release is initially observed at the time of the reward, but once the stimulus becomes a predictor of reward, dopamine is released at the time of the stimulus and not the reward. Together, these findings indicate that the microsensor is responsive on a physiologically relevant timescale.

Pharmacological verification involves the assessment of an evoked signal after the application of an agent known to disrupt the source of the signal. To meet this third criterion, the behaviorally evoked signal at the chronically implanted microsensor was measured before and after an infusion of the $GABA_B$ receptor agonist baclofen (50 ng) into the VTA. Previous work has demonstrated that the majority of dopamine neurons in the VTA express $GABA_B$ receptors, and that activation of $GABA_B$ functionally inactivates dopamine neurons via hyperpolarization[10,11]. Consistent with these findings, food-evoked electrochemical signals were significantly attenuated by intra-VTA baclofen (to $26.0 \pm 24.7$ % of baseline; two tailed paired t-test, $t = 3.062$, $P < 0.05$, $n = 5$) but were not affected following vehicle infusion ($101.5 \pm 21.6$ %; $n = 5$) in the same animals (**Supplementary Figure 4**), again indicating that the signal is dopamine.

The final criterion for the characterization of an *in vivo* signal of interest is independent chemical verification which provides an opportunity to test whether the chronically implanted microsensor can perform at the level of existing methodologies. Rapid changes in dopamine transmission after the presentation of salient stimuli, including reward presentation and reward-predictive cues, have been previously demonstrated with FSCV at acutely implanted electrodes[12,13]. Therefore it is important to verify that comparable chemical signals are observed in the chronically-implanted environment. As demonstrated in **Figure 2c**, phasic signals during reward presentation and in response to reward predictive cues recorded day-to-day at the chronically implanted electrode are extremely consistent with the "snapshots" provided by acutely implanted electrodes at



Nature Methods: doi:10.1038/nmeth.1412

specific time points. Thus, well-characterized recordings from the acutely implanted environment provide independent chemical verification of the data presented with the current approach.

We have presented a comprehensive characterization of the chronically implanted microsensor for the detection of a behaviorally relevant stimulus (food-pellet presentation) using standard signal-identification criteria[2,3] based upon electrochemical, anatomical/physiological, pharmacological and independent verification. Collectively, the findings demonstrate the capability of these chronic microsensors to make chemically selective, subsecond recordings in behaving animals.


1. Wightman, R.M., Kuhr, W.G., & Ewing, A.G. *Ann. N. Y. Acad. Sci.* **473**, 92-105 (1987).
2. Marsden, C.A., Joseph, M.H., Kruk, Z.L., Maidment, N.T., O'Neill, R.D., Schenk, J.O., & Stamford, J.A. *Neuroscience* **25**, 389-400 (1988).
3. Phillips, P.E.M., & Wightman, R.M. *Trend. Anal. Chem.* **22**, 509–514 (2003).
4. Heien, M.L.A.V., Phillips, P.E.M., Stuber, G.D., Seipel, A.T., & Wightman, R.M. *Analyst* **128**, 1413-1419 (2003).
5. Heien, M.L.A.V., Johnson, M.A., & Wightman, R.M. *Anal. Chem.* **76**, 5697-5704 (2004).
6. Marshall, J.F., O'Dell, S.J., Navarrete, R., & Rosenstein, A.J. *Neuroscience* **37**, 11-21 (1990).
7. Garris, P.A., & Wightman, R.M. *J. Neurosci.***14**, 442-450 (1994).
8. Schultz, W. *Neuron* **36**, 241-263 (2002).
9. Pan, W.X., Schmidt, R., Wickens, J.R., & Hyland, B.I. *J. Neurosci.* **25**, 6235-6242 (2005).
10. Wirtshafter, D., & Sheppard, A.C. *Brain. Res. Bull.* **56**, 1-5 (2001).
11. Johnson, S.W., & North, R.A. *J. Physiol.* **450**, 455-468 (1992).
12. Roitman, M.F., Stuber, G.D., Phillips, P.E.M., Wightman, R.M., & Carelli, R.M. *J. Neurosci.* **24**, 1265-1271 (2004).
13. Stuber, G.D., Klanker, M., de Ridder, B., Bowers, M.S., Joosten, R.N., Feenstra, M.G., & Bonci, A. *Science* **321**, 1690-1692 (2008).




Nature Methods: doi:10.1038/nmeth.1412